Article

Biochar from Agro-Forest Residue: Application Perspective Based on Decision Support Analysis

Tsvetelina Petrova [1] , Iliyana Naydenova [1], João Ribau [2] and Ana F. Ferreira [3,*]

1 Technical College-Sofia, Technical University of Sofia, 1000 Sofia, Bulgaria
2 Agência Nacional de Inovação (ANI), 1649-038 Lisboa, Portugal
3 IDMEC, Instituto Superior Técnico, Universidade de Lisboa, 1649-004 Lisboa, Portugal
* Correspondence: filipa.ferreira@tecnico.ulisboa.pt

Abstract: The present work aims at (a) carbonizing agriculture biomass residue; (b) characterizing the obtained biochar; and (c) exploring its potential use for energy/resource recovery purposes. Six types of biomass were carbonized. The biochar was investigated through scanning electron microscopy with energy dispersive X-ray spectroscopy detector, thermogravimetric (TGA), proximate, ultimate, and Brunauer–Emmett–Teller analyses, along with bulk density, pH, electrical conductivity, and salt content measurements. The results served as input data for multi-criteria, multi-objective decision analysis of biochar, aiming to evaluate its best application prospective. The TGA identified two general stages: devolatilization (stage 2: 180–560 °C), and combustion (stage 3: 560–720 °C). The activation energy of stage 2 decreased with an increasing heating rate, but the opposite trend was observed for stage 3. The biochar CO_2 adsorption suggested possible applications beyond energy conversion technologies. The decision support analysis revealed that peach stones, cherry stones, and grape pomace biochar achieved the most promising results for all evaluated applications (biofuel; catalyst; CO_2 sequestration and soil amendment; supercapacitor) in contrast to colza, softwood, or sunflower husks char.

Keywords: biomass; carbonization; biochar characterization; decision support analysis

1. Introduction

The average annual biomass produced in the land-based sectors (agriculture and forestry) of the European Union (EU) is 1466 Mt dry matter between 2006 and 2015 (956 Mt agriculture and 510 Mt forestry, respectively). Some of the biomass should stay in the field to maintain the carbon sink and the other ecosystem services [1].

Currently, biomass residues from agriculture, forest, and food industry are used for different purposes. Portugal is a huge producer of wine. The wine industry generates a significant amount of grape pomace—20–25% of the grape used in wine production [2]. The grape pomace consists of seeds, skins, and stems in different proportions. Bulgaria is well known for having long-term traditions in cultivating agricultural produce, which is usually used for human and animal food as well as raw materials for biofuel manufacturing [3,4]. This Member State is one of the biggest European sunflower producers [5], mainly processing it into sunflower oil. The remaining sunflower husks have pronounced energy potential. In addition, the fruit-growing sector (cherries, peaches, plums, etc.) plays a remarkable role in the Bulgarian industry, as well as the cultivation of wheat and colza [6]. The production of cherries and peaches has increased during the last years [7]. The fruit stones remaining after fruits' processing, together with other types of biomass residue generated by the food industry, are foreseen as possible energy carriers by the Ministry of Energy of Bulgaria [8]. These residues could be converted into solid biofuel, or some of them can be directly burnt, such as fruit stones. Different technologies of biomass conversion are applied depending on the targeted products.

The agriculture biomass can be used in several thermochemical and biochemical conversion processes (gasification, pyrolysis, anaerobic digestion, etc.), obtaining valuable products [9–11]. Recent study proposes biochar (from maple leaf) for the removal of anionic and cationic dyes [12]; others obtain good adsorptive characteristics of biochar of diverse origin [13–15].

The process of carbonization is often used for producing biochar from different feedstocks (e.g., coal, biomass, refuse-derived fuels, sludge, and others). The resulting products typically show increased carbon content and higher calorific value [16,17]. Biomass carbonization at low temperature improves not only its energy content but also facilitates its handling, transportation, and storage. Additionally, carbonized biomass is easy to be ground and, thus, it requires less energy for pulverization [2,18]. Pala et al. [2] studied the hydrothermal carbonization of grape pomace at 175–275 °C and torrefaction (under nitrogen atmosphere at 250 and 300 °C), and obtained mass yield biochar ranging between 47 and 78%. Ronsse et al. [19] investigate biochar from different feedstocks after slow pyrolysis and carbonization. The used biomass was carbonized at four temperatures (300, 400, 600, and 750 °C) and two residence times, 10 min and 60 min. It is observed that the biochar yield for wood, straw, green waste, and algae is 20–25% in the temperature range of 450–750 °C. The authors point out that the biochar yield depends mainly on the residence time, especially at temperatures above 400 °C. Wang et al. [20] report similar temperature dependence during carbonization of palm fiber, where the biochar yield changes from 24 to 18% between 400 and 700 °C. Wystalska et al. [21] produce biochar from sunflower husks at different temperatures (480, 530, and 580 °C), heating time (65 and 120 min), and retention time (10 and 60 min). The authors suggested that the obtained biochar can be used as source of chemical elements, which are important for the plants' growth (Ca, B, Mg, and P). Zabaniotou et al. [22] studied the sunflower shells' utilization in a captive sample reactor at temperatures between 300 and 600 °C and in inert atmosphere (helium). The estimated activation energy (*E*) of the devolatilization stage is 78.15 kJ/mol. The same authors confirmed that the maximum gas yield is obtained at 500 °C, while the maximum oil yield is at 400 °C.

Currently, biochar is of particular interest to a wide range of research fields and economic sectors [23,24]. The properties of biochars are investigated for soil improvement [25–27]. According to [28,29], biochar application is a promising and effective method for remediation of various contaminations including heavy metals in soil. The application of biochar as catalyst for biodiesel production is proposed by [30,31]. Investigations of biochar obtained from pyrolyzed almond shells show encouraging results in producing sustainable and cost-effective electrodes for bioelectrochemical systems, as they perform comparably to carbon felt electrodes [32]. Similar are the findings of Chen et al. [33] who examine walnut shell biochar. The material was used to prepare the microbial fuel cell (MFC) electrode. The authors conclude that the investigated biochar is a promising MFC electrode material.

However, the specific properties of the derived biochar strictly depend on the feedstock used, the chosen conversion technology, and the operating conditions [34]. The products' characteristics are evaluated using different analytical methods and procedures [35], thus, providing valuable data allowing to determine the possible aspect of biochar utilization [36].

According to Waqas et al. [37] and Balat [38], very important advantages of biochar combustion are the reduced emissions of air pollutants and the opportunity for increased fuel diversification. Biomass pyrolysis or carbonization normally reduces the volatile matter by between 30 and 60%, depending on the applied conditions. This considerably influences combustion emissions. Gao X. and Wu H. [39] burned pulverized biochar in a Drop Tube Furnace (DTF) and observed a significant reduction in particulate matter's emissions in comparison to feedstock combustion. Current research is focused on detailed characterization and kinetic analyses of biomass combustion [22,40–43]. Increasing interest in biochar combustion was also identified [44,45]. Biomass is associated as a potential renewable source of energy merely due to its wide availability. However, not only may

energy conversion processes be the best or the most efficient use for any kind of biomasses, but added-value processes may also be a potential option. In this sense, decision support methods become important to unlock the unrevealed potential of bioenergy as stated by the European Green Deal initiative of the European Commission [46].

In this paper, the properties of the obtained biochar produced from agro-forest feedstock were analyzed, aiming to select the best potential application—biofuel, catalyst, for CO_2 sequestration and soil amendment or supercapacitor development—since those are known to be potentially efficient applications [47–50].

Decision analysis has been used in order to assess the best application according to the properties of the obtained biochar. The use of a multi-criteria decision approach demonstrates its strength in the selection of the most efficient biomass/biochar along with the conversion routes of biorefinery value chains, considering the detailed proprieties of biomass and a life cycle impact perspective [51]. Decision methods were also focused on finding the best option to produce electricity, considering the pathway life cycle emissions and energy efficiency [52]. In another investigation on energy conversion, with an accent on biofuel, decision techniques [53] were applied to analyze the technology maturity, conversion efficiency, costs, emissions, and land requirement. However, none of the mentioned studies considered the biomass properties, biomass carbonization, and different product characterization as well as obtaining their application perspective based on a multi-criteria decision approach.

The main goal of the present study was (a) to carbonize biomass residue; (b) to characterize the obtained biochar; and (c) to explore its potential application as biofuel, catalyst, supercapacitors, or as CO_2 sequestration and soil amendment—since those are known to be probable efficient applications [47,48,50]. To this end, six different types of biomass residue (agro-forest) were studied, originating from two European countries with well-established agricultural traditions. The biomass residue was investigated prior to the present research, applying the following methods: proximate, ultimate, ash, lignocellulosic, and HHV analyses. The residue was carbonized in an inert atmosphere (nitrogen) using a Horizontal Tube Furnace (HTF), in accordance with Ferreira et al. [54]. The derived biochar was examined through a set of physical and chemical analyses. In focus were the following global parameters: (i) the effect of feedstock on biochar yield; (ii) biochar thermal decomposition in air, its stability, and kinetics; (iii) biochar characterization using proximate, ultimate, EDS, and HHV analysis; morphology and specific surface area; technical parameters, such as bulk density, pH, EC, and salt content; (iv) application prospective, based on a multi-criteria decision approach.

A previous study by the authors applied multi-criteria decision analysis to evaluate the best application of biochar produced from grape pomace biomass, considering the measured biomass characteristics and conversion process properties [54]. The decision focused on the carbonization conditions and the potential use of the products for biofuels, biofertilizer, or catalysts for biofuel production. In the present investigation, the authors used similar methods but assessed a larger number of process variables, thus increasing the accuracy of the methods. Moreover, a greater variety of biomass sources was examined herein. The chosen decision methods—Pareto front evaluation and compromise programming—are mathematical techniques typically used in multi-criteria, multi-objective decision analysis, as well as in the optimization field.

2. Materials and Methods

2.1. Used Biomass

Six different types of biomass residues were used in this study—grape pomace, cherry stones, peach stones, colza, sunflower husks, and softwood (containing raw carpwood and bark). The grape pomace biomass was provided by a local Portuguese wine producer of Agrovil, while the other biomass was from Bulgaria. The fruit residues were from "Fructo Sliven" Joint-Stock Company (Sliven, Bulgaria) and the colza was delivered by the Agricultural production and consumer cooperative in Batak town. The sunflower husks

and the softwood were supplied by Rosina Oil Ltd. (Resen, Bulgaria) and Axel Trade 2009 LTD, Samokov town, Bulgaria, respectively.

The proximate, ultimate, and ash analyses as well as the higher heating values of the biomass residues are published elsewhere [1–3]. The lignocellulosic composition of the biomass investigated in the present study is published in [2,3]. Herein, the lignin content corresponds well with the literature data [4–8].

2.2. Horizontal Tube Furnace and Test Conditions

The carbonization was performed in electrically heated HTF shown in Figure 1. The apparatus has an alumina recrystallized tube, with a length of 55 cm and an inner diameter of 4 cm, and operates at a maximum temperature of 1300 °C. The wall temperature is continuously monitored by thermocouple type S. The experiments were carried out at a wall temperature of 500 °C, at a heating rate of 33 °C/min, and an inert atmosphere (nitrogen), with a residence time of 1 h and nitrogen flow rate of 1 L/min. The mild heating conditions aimed at producing biochar with multiple application potential [3]. Two ceramic crucibles were placed in the middle of the HTF, each of them containing sample mass of approximately 1 g. The used biomass was ground and sieved to obtain a particle size below 1 mm. For this purpose, a sieve with an aperture size of 1 mm was used, through which 95% by mass of the ground material passes. The HTF was purged for 20 min with nitrogen, assuring that the carbonization process will be conducted in absence of oxygen. When the wall temperature reached 500 °C, the samples were heated for one hour and then cooled down into the HTF under nitrogen atmosphere.
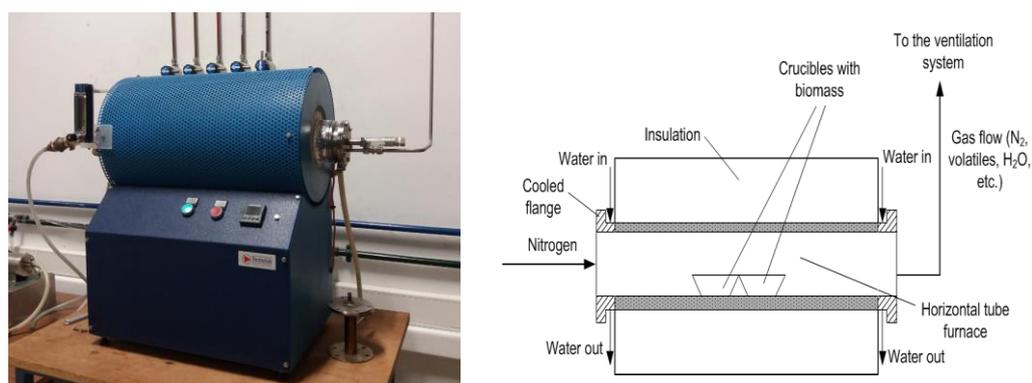

Figure 1. Experimental apparatus and scheme of the HTF.

2.3. Experimental Methods Used for Biochar Characterization

Thermogravimetric analysis (TGA) of the obtained biochar was carried out with TA Instruments SDT 2960 V3.0F (New Castle, DE, USA). The apparatus has a weighing precision of ±0.01% and sensitivity in the mass measurements of 0.1 mg. The thermogravimetric tests were performed using a sample weight between 7 to 11 mg, depending on the density of the biomass used [39]. Each biochar sample was heated from 25 to 1100 °C, in air and at four heating rates, namely 10, 20, 30, 40 °C/min. The temperature was measured with an experimental uncertainty of ±1 °C.

The biochar morphology was examined with the use of a conventional Scanning Electron Microscope (SEM)—Hitachi, (Tokyo, Japan) S2400 model, with an acceleration voltage of 20 kV, with digital image acquisition with Esprit software, with Bruker (Billerica, MA, USA) coupled light element EDS SDD detector. The chemical composition was depicted through an Energy Dispersive X-ray Spectroscopy (EDS) detector.

The specific surface area of the obtained biochar was estimated through the Brunauer–Emmett–Teller (BET) method. To this end, the samples were degassed in apparatus Flow-Prep 60, Micromeritics (Norcross, GA, USA), under continuous flow of helium. FlowPrep 60 combines flowing gas and a vacuum with heat to remove atmospheric contaminants, such as water vapor and adsorbed gases, from the sample's surface and pores. After this

preparation, the samples' specific surface areas were measured through TriSTAR II 3020, Micromeritics. It calculates BET specific surface area by measuring the gas adsorption of carbon dioxide (CO_2).

Biochar proximate, ultimate, calorimetric, and bulk analyses were carried out following the standards and procedures applied for the biomass analysis [40–43]. The parameters pH, electric conductivity (EC), and salt content were determined according to [44], using a multi-parameter measuring device (T; pH; EC and salt content) of type Combo HANNA Instruments HI 98129 (Woonsocket, RI, USA). It was equipped with a combined pH electrode and calibrated with pH-buffer solutions (HI 73127) having pH = 4, 7, and 10 (20 mL) and EC-buffer solution (HI 70031P) having an *EC* of 1413 µS/cm (20 mL). The salt content was obtained in ppm. The biochar aqueous extracts were prepared with deionized water in a ratio of 1:20. The sample extraction was carried out in graduated tubes, shaking the samples for 1 h.

2.4. Kinetic Analysis

The kinetic parameters (activation energy, *E*, and pre-exponential factor, *A*) were calculated from the TGA data using a model based on the Arrhenius equation [39,45,46].

The mass conversion, α, was determined through the following equation:

$$\alpha = \frac{m_i - m_T}{m_i - m_f} \tag{1}$$

where m_i is the initial mass at time t = 0 s; m_T—the mass at the temperature *T*; m_f—the final mass of the sample.

The biochar thermal decomposition was modeled using a first-order mechanism based on the Coats–Redfern method [37,39,47]. Thus, Equation (1) can be expressed as Equation (2):

$$\frac{d\alpha}{dt} = A.e^{-\frac{E}{R.T}} \cdot f(\alpha) \tag{2}$$

where *f(α)* is the hypothetical model of the reaction mechanism and *R* is the universal gas constant.

Several studies used this model based on first-order mechanism because it produces the best correlation coefficient for the lignocellulosic biomass combustion process, considering that the composition of the biomass does not influence the overall reaction mechanism of the lignocellulosic biomass oxidation. However, several works have been developed to identify the best model for kinetic analysis [19,29].

2.5. Decision Support Analysis

Biochar has versatile physicochemical properties which proposes its use for a diversity of potential applications. Not only the properties, but the conversion process can also be more beneficial for specific utilizations. At present, four potential applications have been studied: the use of biochar as biofuel, as catalyst, for CO_2 sequestration and soil amendment, or for supercapacitor development.

Although the maturity level of industrial biofuel production is not at a full commercial stage, e.g., issues with continuous yield capacity, the biofuel pathway is still one of the most attributive to biomass due to its energy content [48]. On the other hand, catalyst processes are known to use carbon-based materials, where biochar can have its role. In addition, biochar's physical and chemical properties can be adjusted to best fit a specific application [49]. Similar features of biochar can be applied to other processes, such as CO_2 sequestration and soil amendment, or supercapacitor development due to its large specific surface area, porous structure, surface functional groups, and high mineral content [50,51].

In the present work, different criteria were selected for each of the explored application opportunities. Thus, the analyzed criteria were the ones that recurrently appear to have the highest influence in each application, balanced by a less complex/expensive characteriza-

tion. The decision problem was based on the definition of the process conditions that are best in terms of proposing the biochar utilization as a biofuel, catalyst, CO_2 sequestration, and soil amendment product, or for supercapacitor development, given the decision criteria shown in Table 1.

Table 1. Decision variables for each application.

Biofuel (12 Variables)			Catalyst (6 Variables)			CO_2 Sequestration and Soil Amendment (9 Variables)			Supercapacity (9 Variables)		
Variable	Decision Goal	Best Value	Variable	Decision Goal	Best Value	Variable	Decision Goal	Best Value	Variable	Decision Goal	Best Value
Moisture (%)	lower	4.49	EDS/Content (%) of C, K, Ca, P	higher	82.62%C, 10.05%K, 8.20%Ca, 2.27%P	EDS/Content (%) of C, K, Ca, P	higher	82.62%C, 10.05%K, 8.20%Ca, 2.27%P	EDS/C, K, Ca, P Content (%)	higher	82.62%C, 10.05%K, 8.20%Ca, 2.27%P
Ash (%, db)	lower	1.29									
HHV (MJ/kg)	lower	33.34									
Ashes (%)	higher	1.36	Ultimate analysis/Content (%) of C	higher	82.35	Ultimate analysis/Content (%) of C	higher	82.35	Ultimate analysis/Content (%) of C	higher	82.35
E (kJ/mol) stage 2—10, 20, 30, 40 °C	lower	94.1, 99.71, 84.4, 80.2	Specific surface area (m²/g)	higher	331.62	Specific surface area (m²/g)	higher	331.62	Specific surface area (m²/g)	higher	331.62
E (kJ/mol) stage 3—10, 20, 30, 40 °C	lower	96.73, 100.34, 105.4, 99.5				Bulk density (g/cm³)	higher	0.4455	Bulk density (g/cm³)	higher	0.4455
						EC (μS/cm)	higher	1960	EC (μS/cm)	higher	1960
						pH	higher	11.08	Salt content (ppm)	higher	980

Among all tested types of biochar, several possible solutions were found fitting to the applications, but there was no one-fits-all solution, e.g., a decision technique is necessary to choose the preferred process in accordance with the variables. The decision analysis was performed with the following methods: Pareto dominance analysis and an approach of compromise programming [3,52].

2.5.1. Pareto Dominance Analysis

The concept of dominance as a viable approach for comparing several criteria or objectives was first introduced in solving multi-objective optimization problems [52].

In a decision problem, the complexity exists when finding a solution that is not exclusively dependent on one criterion (e.g., search for the solution with the highest HHV), but is rather dependent on several criterion simultaneously. In such cases, there can be better solutions in terms of one criterion that are worse in another. Thus, the question is which is preferential. Normally, several solutions are possible, but in a trade-off perspective. However, it is possible to analyze whether a solution is better than others with respect to several criteria, or in most criteria, and this relies on the definition of dominance. In a set of N solutions $x_n = \{x_1, x_2, \ldots, x_N\}$ of a problem with p decision criteria $f_p = \{f_1(x_n), f_2(x_n), \ldots, f_M(x_n)\}$, solution x_1 dominates solution x_2 if and only if x_1 is not worse than x_2 in all criteria and x_1 is strictly better than x_2 in at least one criterion (Equation (3)).

$$x_1 \preceq x_2 \, iff \left\{ f_i(x_1) \leq f_i(x_2) \forall_i \in 1, \ldots, p \exists_j \in 1, \ldots, p f_j(x_2) < f_j(x_2) \right. \tag{3}$$

The signs $\leq$ and $<$ (Equation (3)) represent the desire to minimize all the criteria (e.g., for simplicity, all criteria in Table 1 were mathematically translated into minimization criteria, whereas for the maximization of HHV, the inverse was applied).

A solution x_n is called non-dominated if it is better in all criteria than all other solutions. On the other hand, a solution has weak dominance if it is better in at least one criterion or strong dominance if it has better or equal results in all criteria. The goal of this paper was to find the set of variables that produces the best solutions possible for the specified applications, e.g., non-dominated (or the least dominated possible).

2.5.2. Compromise Programming Approach

Assuming that there is a desired set of variables, as the best possible (Table 1), the method of compromise programming privileges a solution that is closer to such a scenario. The closeness is defined by a metric distance (d_n), measured by a specific vector—the Euclidean distance—between a solution x_n and a reference point in the solutions space that represents that perfect scenario.

The reference point, the fictitious solution representing the best possible scenario, is given by the coordinates of the preferred values (lowest or highest possible) of all the criteria presented for each product—biofuel and catalyst (see Table 1). For the sake of simplicity, all criteria are translated into minimization problem. The preferred solution will be the one that has the shortest distance for this reference solution (Equation (4)).

$$d_n = \left[\sum_{m=1}^{M} |f_m(x_n) - z_m|^p \right]^{1/p}$$ (4)

where $f_m(x_n)$ is the value of solution n in the criterion m, M is the number of all solutions, z_m stands for the result of the reference solution in criterion m, and p is the number of criteria—different for each product—biofuel (12), catalyst (6), CO_2 sequestration (9), supercapacitor (9).

3. Results and Discussion
3.1. Biochar Yield

The relative mass yield of the biochar, obtained in the present work, and the relevant literature data are summarized in Table 2.

Table 2. Yield and EDS analysis of biochar derived from different feedstock.

Type of Biomass	Colza	Cherry Stones	Peach Stones	Grape Pomace	Softwood with Bark	Sunflower Husks
Biochar derived from different feedstock						
Biomass (g)	1.05	1.06	1.05	1.06	1.05	1.03
Biochar (g)	0.30	0.31	0.34	0.37	0.28	0.33
Biochar yield (%), present work	28.66 ± 0.14	29.24 ± 0.73	32.26 ± 1.32	35.07 ± 0.40	26.35 ± 1.09	31.48 ± 0.77
Biochar yield (%),	28–30 [36]	27.50 [14] 27.00 [13]	33.56 [11]	39.68 [37]	27.00 [38]	31.59 [39]
EDS analysis						
Carbon (%)	78.67	76.71	76.17	73.94	82.62	65.42
Oxygen (5)	15.75	14.14	19.41	17.08	16.66	19.17
Ash (%)	5.58	9.14	13.32	8.99	0.73	15.41
Descending order of ash component (%)	K (2.88) > Ca (2.35) > Na (0.16) > Mg (0.15) > S (0.03) > P (0.01)	K (4.30) > P (2.27) > Ca (1.58) > Mg (0.99) > Si (0.01)	K (10.05) > Si (1.52) > Ca (0.45) > Al (0.43) > Fe (0.40) > Mg, P (0.21) > S (0.04) > Na (0.02)	K (4.23) > Ca (2.97) > P (0.80) > Mg (0.32) > Si (0.28) > Al (0.16)	Si, K, Al (0.06) > Ca (0.55)	Ca (8.20) > K (6.27) > Mg (0.43) > S (0.42) > Na (0.05) > P (0.04)

The results expressed in % were obtained using Equation (5):

$$Y_m = \frac{m_{biochar,fin}}{m_{biomass,init}} \cdot 100\%$$ (5)

where Y_m is the relative biochar yield, $m_{biochar,fin}$ is the measured mass of the biochar, and $m_{biomass,init}$ is the initial mass of the biomass residue prior to the carbonization process.

The grape pomace showed the highest biochar yield with $35.07 \pm 0.40\%$, while the lowest one was derived from the softwood, $26.35 \pm 1.09\%$. Similar results were reported in [55,56]. The presently obtained biochar yield, derived from sunflower husks, softwood, peach and cherry stones, and colza is in agreement with the results from other experiments [18,21,53,56,57] (Table 2). An observable difference was found only for the grape pomace samples, which was dedicated to the variations in the biomass composition (seeds/skin/stems).

3.2. Thermogravimetric Analysis of Biochar

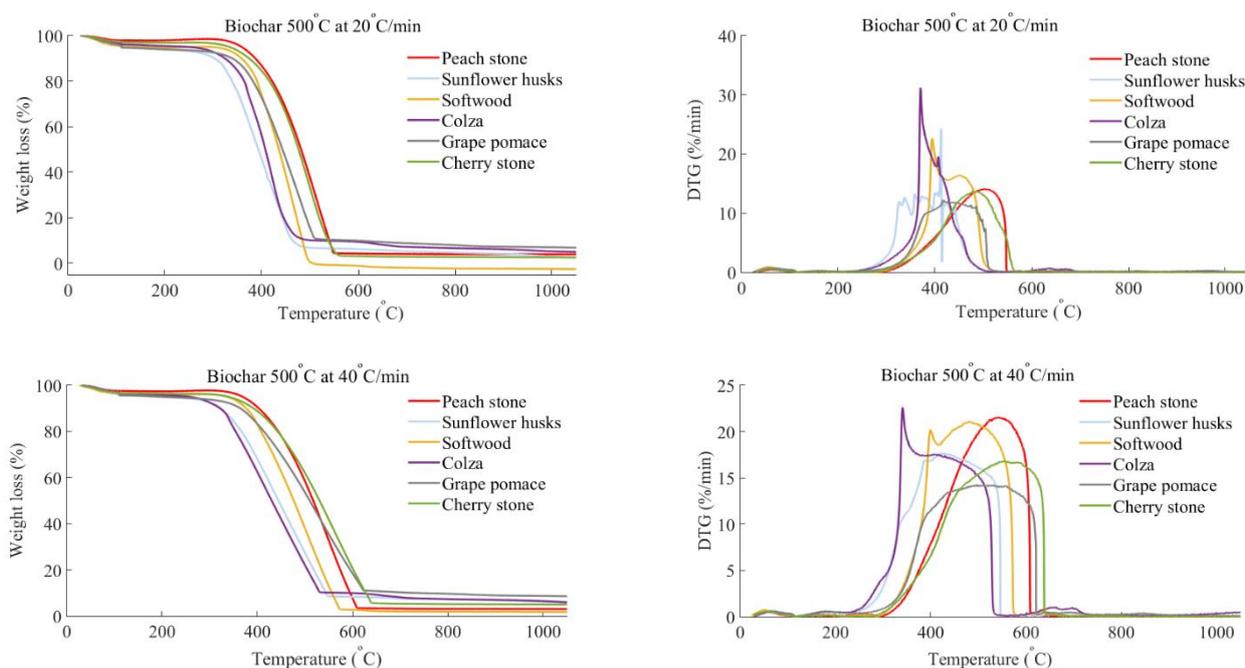The effects of the feedstock and the heating rate on the TGA are expressed in Figures 2 and 3.

Figure 2. Effect of feedstock on the oxidation of six types of biochar at given heating rate (20 and 40 °C/min), TGA and DTG in air.
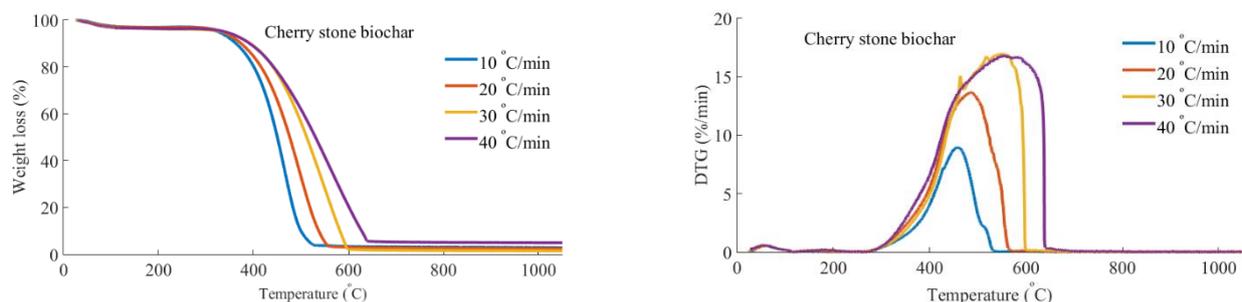

Figure 3. Effect of heating rate on cherry stone biochar oxidation, TGA and DTG in air.

The maximum mass reduction of about 98 wt. % was determined for the biochar derived from softwood carbonization. The TGA revealed two-staged conversion: devolatilization (stage 2) and char combustion (stage 3). Stage 1, corresponding to the water mass loss up to 180 °C, was not considered because the samples showed low moisture content. Due to the reduced biochar's content of volatiles (Table 1), stage 2 was weakly expressed in comparison to the TGA of biomass [3] and occurred in the temperature range from 180 to 560 °C. Stage 3 took place between 400 and 720 °C for all studied biochar types and heating rates.

Comparison of the DTG data for colza, sunflower husks, and softwood revealed that their maximum mass reduction was between 370 and 400 °C, which corresponds with the high percentage of cellulose in their feedstock composition. The process of thermal decomposition of these types of biochar required less energy to initiate the combustion process than the one obtained from cherry and peach stones.

The DTG curves of peach and cherry stones and grape pomace showed their maximum at 400–500 °C and released a higher amount of heat during the combustion. The effects were associated with the highest lignin content, reported in [2,3], and the highest HHV of the biochar, derived from kernel/seed-containing biomass.

The weight loss rate decreased when increasing the heating rate. Both TGA and DTG curves were slightly shifted to the right with an increase in heating rate (Figure 3). The same effects were described by Fan et al. [37]. The authors explain the appearance of this phenomenon through the stronger thermal shock occurring in a short time and a greater temperature gradient between inside and outside that the sample develops. When the heating rate increases, the temperature of the biomass particle drops more abruptly, showing greater energy absorption [58].

3.3. Kinetic Analysis

Comprehensive kinetic analysis was carried out, applying the model described in Section 2.4, and considering two-staged combustion: biochar devolatilization (stage 2) and combustion (stage 3). Generally, all six types of biochar showed similar kinetic profiles. The calculated kinetic parameters and their corresponding correlation factors R^2 are given in Table 3.

Table 3. Calculated kinetic parameters and correlation factor R^2.

Biochar	Colza	Cherry Stones	Peach Stones	Grape Pomace	Softwood	Sunflower Husks
Heating rate 10 °C/min						
Stage 2						
E (kJ/mol)	95.21	111.9	119.2	125.2	131.7	94.1
A (1/s)	1.44×10^5	2.69×10^6	6.06×10^6	1.19×10^8	8.92×10^7	9.1×10^4
R^2	0.9906	0.9934	0.9904	0.9900	0.9913	0.9848
Stage 3						
E (kJ/mol)	96.73	209.4	305.4	148.9	134.97	274.3
A (1/s)	2.69×10^6	1.21×10^{16}	2.35×10^{19}	5.40×10^8	3.7×10^7	1.42×10^{11}
R^2	0.9782	0.9935	0.9868	0.9926	0.9543	0.9703
Heating rate 20 °C/min						
Stage 2						
E (kJ/mol)	99.71	119.5	112.9	125.7	149.7	114.9
A (1/s)	1.20×10^6	1.79×10^7	2.31×10^6	7.62×10^7	5.86×10^9	2.62×10^7
R^2	0.9907	0.9826	0.9911	0.9944	0.9928	0.9914
Stage 3						
E (kJ/mol)	100.34	208.9	231.9	172.3	196.9	166.8
A (1/s)	2.514×10^5	2.76×10^{12}	3.03×10^{13}	8.47×10^9	9.92×10^{11}	1.85×10^{10}
R^2	0.9833	0.9645	0.9684	0.9909	0.9931	0.9674
Heating rate 30 °C/min						
Stage 2						
E (kJ/mol)	86.3	110.6	84.4	91.6	160.9	96.9
A (1/s)	4.45×10^4	3.73×10^6	6.16×10^3	4.64×10^4	6.61×10^{10}	3.32×10^5
R^2	0.9976	0.9948	0.9862	0.9953	0.9929	0.9831

Table 3. *Cont.*

Biochar	Colza	Cherry Stones	Peach Stones	Grape Pomace	Softwood	Sunflower Husks
Stage 3						
E (kJ/mol)	478.30	118.1	105.4	283.2	157.1	276.2
A (1/s)	7.26×10^{31}	3.67×10^5	7.95×10^3	4.25×10^{16}	9.3×10^8	4.33×10^{17}
R^2	0.9925	0.9919	0.9828	0.9933	0.9901	0.9775
Heating rate 40 °C/min						
Stage 2						
E (kJ/mol)	102.4	116.6	86.3	85.6	86.9	80.2
A (1/s)	4.39×10^6	1.62×10^7	7.14×10^3	1.97×10^4	1.32×10^4	1.08×10^4
R^2	0.9951	0.9915	0.9909	0.9943	0.988	0.9846
Stage 3						
E (kJ/mol)	112.6	109.4	463.5	99.5	562.9	429.9
A (1/s)	9.76×10^5	1.21×10^5	5.52×10^{26}	9.87×10^3	1.12×10^{34}	4.99×10^{26}
R^2	0.9769	0.9934	0.9833	0.9935	0.9759	0.964

The oxidation of the currently examined biochar showed high E values, which resulted from the high thermal resistance of the feedstock's main constituents (hemicellulose, cellulose, and lignin). Limited numbers of references on biochar oxidation were found in the literature [38,59,60]. The presently obtained biochar oxidation kinetics were compared with literature data for the stage char oxidation of similar types of biomass, burnt under comparable experimental conditions. López-González et al. [36] reported E of 126 kJ/mol to 167 kJ/mol at a heating rate between 10 and 40 °C/min in case of fir wood oxidation. In parallel to the current study, the authors used the Coats–Redfern method for first-order reaction. In the present experiment, the obtained E for softwood biochar oxidation was 134.97 and 562.9 kJ/mol at the same heating rates. Increasing the heating rate led to higher E in both studies. A similar trend was observed when comparing the present results with those reported by Botelho et al. [61]. The authors evaluate the combustion characteristics of raw and torrefied grape pomace (200–300 °C) in a thermogravimetric analyzer (using a heating rate of 10 °C/min) and in DTF, at 1100 °C. They report an apparent E of 84.9 and 85.2 kJ/mol for the devolatilization (assumed to resemble stage 2 of the present study), whereas the E values for the char oxidation (stage 3) were 137.5 and 109.2 kJ/mol for the raw and the torrefied grape pomace, respectively.

3.4. SEM and EDS Analysis

Figure 4 shows SEM images of all biochar types, expressing the particles' morphology and structure.

Carbonization disrupts the smooth structure of the biomass, creating cracks and pores on the biochar surface, and fragmentation of particles (smaller and spherical particles) with the temperature increase [62]. The shape of the biochar particles derived from peach and cherry stones was rounder and had higher porosity. Colza and softwood showed the largest particle size.

The EDS analysis showed that the biochar derived from softwood had the highest carbon content (82.62%), while the lowest value was obtained from the sunflower husks (65.42%). The highest and the lowest oxygen content were in peach stone (19.41%) and cherry stone (14.14%), respectively. The EDS elemental composition for all biochar types is summarized in Table 2.

The biochar carbon content (EDS analysis, Table 2) corresponds with the data obtained in the present ultimate analysis (Table 4). The data for sunflower husks and grape pomace also correspond well with the ultimate analysis, presented by Colantoni et al. [63]. The authors reported 72.1% of carbon in the sunflower husks and 73.77% in grape pomace biochar.
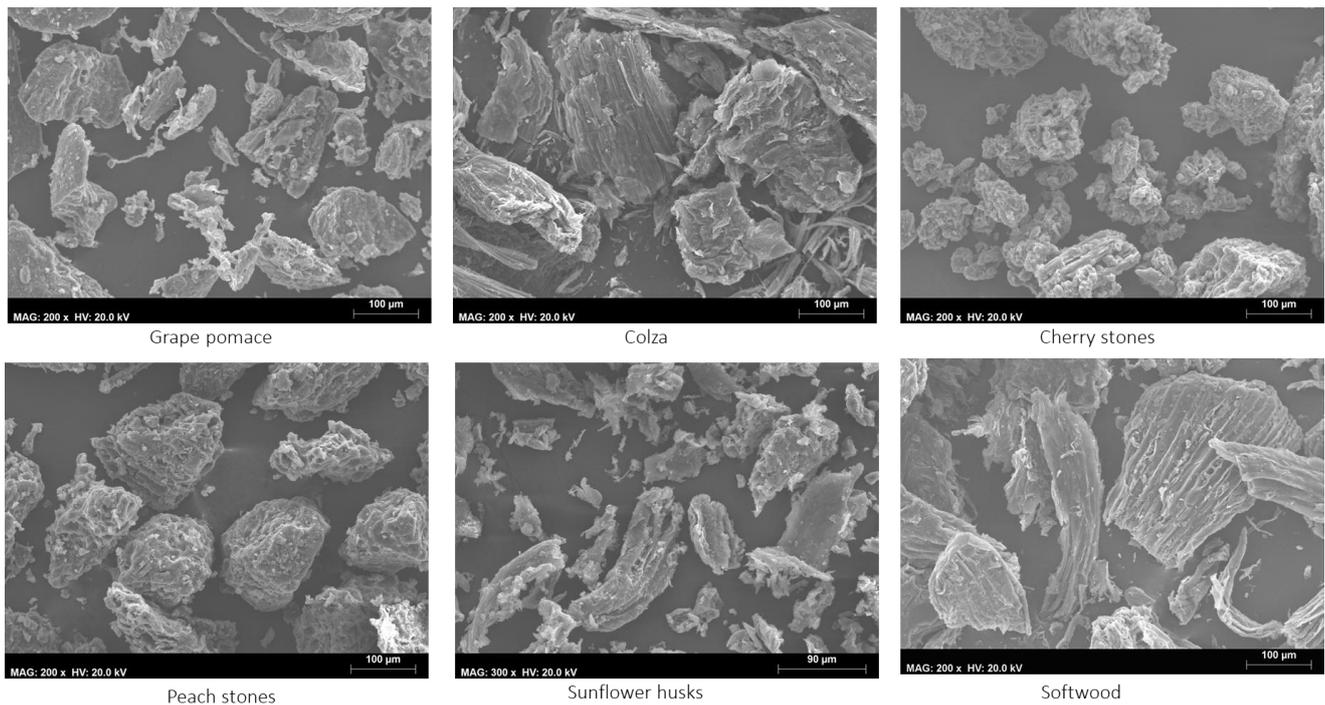
Figure 4. SEM images of the biochar morphology.

Table 4. Biochar characteristics.

			Biochar			
	Colza	**Cherry Stones**	**Peach Stones**	**Grape Pomace**	**Softwood**	**Sunflower Husks**
Proximate analysis (wt. %)						
Moisture	5.32	4.49	4.95	2.84	5.38	9.33
Ashes (db)	7.08	4.47	1.92	12.44	1.29	4.83
Volatile matter (db)	32.10	25.86	30.57	17.91	40.49	44.13
Fixed carbon * (db)	55.51	65.18	62.57	66.81	52.85	41.71
Ultimate analysis (wt. %, db)						
C	73.52	67.01	81.56	77.61	82.35	76.76
H	3.66	3.22	3.61	3.52	3.78	3.50
N	1.97	4.28	<0.10	2.64	0.97	2.24
O*	8.25	16.33	7.66	0.75	6.04	3.13
S	<0.10	<0.10	<0.10	<0.10	<0.10	<0.10
Cl	<0.10	<0.10	<0.10	<0.10	<0.10	<0.10
HHV, MJ/kg	24.94	28.62	33.34	28.11	30.88	31.05
Specific surface area (m^2/g), S$_{BET}$	252.30	265.74	306.72	293.27	331.62	278.25
Bulk density (g/cm^3)	0.1585	0.4455	0.4301	0.3737	0.2028	0.2700
pH	9.70	9.55	9.10	11.08	8.38	9.93
EC (µS/cm)	1015	372	84	1960	56	897
Salt content (ppm)	508	186	42	980	28	448

* by difference.

3.5. Biochar Characterization Using Proximate, Ultimate, Calorimetric, BET, and Combined pH/EC Analyses

The results from biochar proximate, ultimate, and calorimetric analysis are summarized in Table 4.

The biochar, derived from biomass containing kernel, showed the highest fixed carbon content, although the effect cannot be directly related to the concentrated carbon

content. The descending order of the fixed carbon per biochar type is as follows: grape pomace > cherry stones > peach stones > > colza > softwood > sunflower husks. As expected, the opposite trend was observed regarding the content of volatile matter. Figure 5 shows the Van Krevelen diagram, according to Van Krevelen and Te Nijenhuis [64], and Misse et al. [65], of the used raw biomass and the obtained biochar.
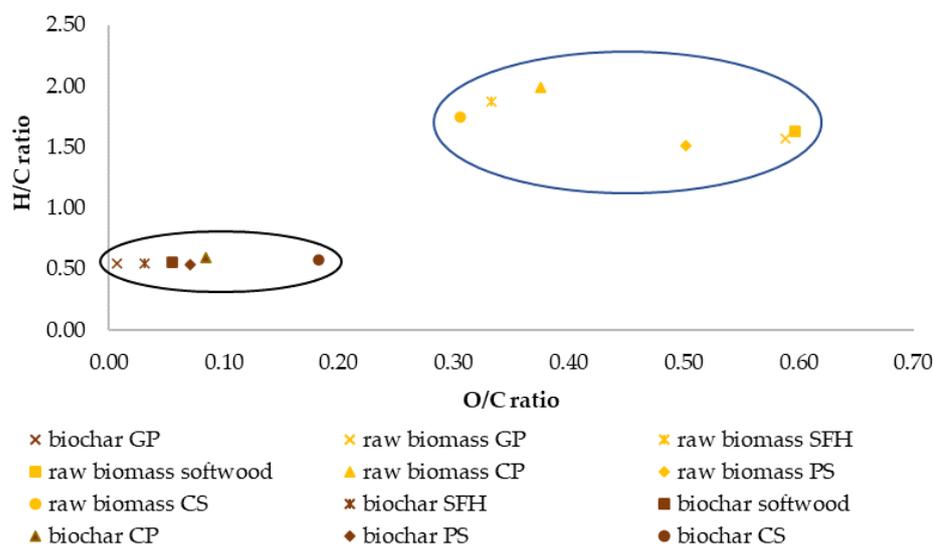

Figure 5. Van Krevelen diagram of the used raw biomass and the obtained biochar.

The comparison of the hydrogen/carbon (H/C) and the oxygen/carbon (O/C) atomic ratio was considered in order to verify the elements' selective loss during the process of dehydration and carbonization [66].

Biochar showed considerably lower H/C, and O/C ratios. According to Waqas et al. [67], the fuels with low H/C and O/C ratios are preferable due to their low smoke, water vapor production, and energy losses. The H/C ratio is often seen as an indicator for carbon stability in biochar [68], which together with the O/C ratio is directly associated with the aromaticity, biodegradability, and polarity of biomass and biochar [66,69]. According to other authors [62,66,69,70], the higher the carbonization temperature is, the lower the observed H/C and O/C ratios are in the resulting biochar samples.

The conversion of agricultural biomass residue to biochar in pyrolytic conditions is proposed as a promising option for feedstock utilization for various sustainable purposes such as a substitution of renewable and environment-friendly energy source [38,71], e.g., for household briquette production [72]. Expectedly, the measured biochar HHV (Table 4) increased on average by 30–50% in comparison to the biomass; the effect was observed also in [38,71,73]. The biochar HHV, proximate, and ultimate analyses confirmed the conclusion of Angin [74], concerning its considerable potential to be used as a renewable energy carrier. However, the biochar thermal and surface stability and reactivity are dependent on the feedstock type and conversion temperature [75].

Recently, in focus is the biochar's prospect of becoming a low-cost sorbent for CO_2 capturing [38]. Waqas et al. [67] investigated the potential of biochar as a fuel and catalyst in the context of different energy recovery technologies.

The experimentally measured specific surface area in m^2/g (S_{BET}), obtained from the CO_2 adsorption at 0 °C, bulk density, pH, EC in μS/cm, and salt content in ppm are summarized in Table 4. The S_{BET} values obtained in the present work were in line with data reported in similar experiments. For instance, Manyà et al. [76] investigated biochar derived from vine shoots. The authors use biomass with particle sizes in the range of 0.1–1.0 cm diameter and 1.0–3.5 cm long, which is pyrolyzed in a packed-bed reactor at peak temperature of 600 °C and at an absolute pressure of 0.1 MPa. They report the biochar's specific surface area of 228 m^2/g which is calculated from CO_2 adsorption at 0 °C.

The recently measured EC varied in a wide range (from 56 to 1015 μS/cm, Table 4), and typically correlated with the total salt content. The results are in accordance with an independent study, reporting variations in biochar EC from 70 to 13,800 μS/cm.

All six types of the currently obtained biochar showed alkaline pH—from 8.38 to 11.08. Waqas et al. [67] suggested that the biochar alkaline pH could improve (increase the efficiency of) some processes of energy recovery technologies, such as anaerobic digestion of biologically degradable feedstock—e.g., neutralizing the natural acidic effect of such processes and, thus, enhancing the subsequent processes leading to biogas generation.

3.6. Decision Analysis

Independent studies investigate the significance of the ash content and ash-forming elements of biomass envisaged to be used as solid biofuels [77,78]. Vassilev et al. [77] identify correlations and associations among the ash yields and contents of the general ash-forming elements of a huge variety of biomass. Thus, the origin and the role of these elements (grouped as follows: (1) Si-Al-Fe-Ti, (2) Ca-Mg-Mn, and (3) K-P-S-Cl-Na) are determined along with the benefits and the obstacles of their associations for biofuel combustion. For instance, the enrichment of elements from group (3) is generally associated with the most critical technological and environmental challenges during biomass thermochemical conversion.

The results from the decision support analysis, based on the experimentally measured biochar characteristics, are shown in Tables S1–S4, Supplementary material. Table S1 presents a summary of the results, obtained in terms of biochar potential application as biofuel. The biochar from cherry stones showed the highest potential application as fuel since most of its parameters dominated among the rest of the investigated biochar (number of weak domination events—meaning that cherry stones have better values in 34 situations or in single variables comparison). It showed the most beneficial balance between all parameters reading the distance metric. However, both feedstock and biochar appeared rich in K and P, which according to Vassilev et al. [77] is a good reason for exploring other utilization pathways. In this point of view, independent studies consider biochar as valuable energy carrier, suitable not primarily for direct combustion but rather as a resource or even additive that facilitates the production of liquid or gaseous biofuels [79].

The results from the decision support analysis regarding the possible char application as catalyst are generalized in Table S2, Supplementary material. In this case, grape pomaces appear to have the highest potential, closely followed by peach stones and cherry stones. The conclusion is based on the obtained higher number of domination events, balanced by the distance metric, which seems to be concurrent. Although peach stones dominated in most solutions, it is the cherry stones and grape pomace that achieved better balance among all variables. Both peach stones and grape pomace can be considered the most advantageous for this application. Waqas et al. [67] provided a detailed literature review and experimental research focused on the application opportunities of biochar as a catalyst suitable for various processes. The authors suggest that biochar can act as a promising low-cost adsorbent for CO_2 capturing due to its highly porous structure and sorptive capacity. They further propose the subsequent conversion of the absorbed CO_2 to fuel, although detailed research is required on the process parameters and kinetic mechanisms that enhance the catalytic conversion of CO_2 to biofuels. Mohamed et al. [80] investigate biomass-derived CaO sorbent for CO_2 capture and conclude that the examined material is suitable for producing CO_2 adsorbents. All six types of biomass analyzed in the present study showed a relatively high content of CaO.

Conder et al. [81] summarize detailed studies on currently investigated carbon-based materials, obtained by biomass carbonization and/or activation. The authors state that activated carbons, known for having versatile properties (e.g., specific surface area, significant porosity, heteroatoms in their graphene matrix, etc.), are highly valued materials for the production of electrochemical capacitors.

According to [82], each biochar is unique, having different chemical and physical properties which depend on the feedstock and the applied technology/operating parameters for biomass conversion. Moreover, the use of biochar as soil amendment is generally a highly challenging issue due to the very strict regulations for the biochar contents of major and trace elements, feedstock origin, the choice of its conversion technology, and many other obstacles [83], which may suggest some biochar as being merely a waste or hazardous material rather than having soil amendment purposes.

Racioppi et al. [84] investigate the response of ancient and modern wheat varieties to biochar application as soil amendment. The authors observed that the addition of biochar affects soil properties as follows: it increases the content organic matter, pH, and the content of phosphorus (P), potassium (K), and sulfur (S) in the soils as well as the shoot and root biomass of wheat. However, biochar can improve soil health and crop productivity, depending on the rate of wood biochar and fertilizers addition, but these parameters should be studied with respect to the properties of the soil, the agricultural plants, the biochar origin, and production technology.

Table S3, Supplementary material, shows results from the currently performed decision support analysis, aiming to estimate the biochar potential application for CO_2 sequestration and soil amendment processes. The grape pomace expressed the highest potential for application in CO_2 sequestration and/or soil amendment processes, dominating over a large number of events. Although the metric distance was worse than for cherry stones, grape pomace indicated good balance between all variables. Thus, grape pomace was considered as the most advantageous for this application, followed by peach stones and cherry stones.

Table S4, Supplementary material, reports the results from the decision support analysis for supercapacitor process application. This analysis showed solutions that are very similar to the ones encountered in CO_2 sequestration analysis, where the salt content was used instead of pH. Consequently, grape pomace was again the most suitable for this application, followed by peach stones and cherry stones.

The results revealed that no solution is completely dominant because no non-dominated solutions were identified. All solutions accounted for 0% of full domination in all parameters in each application. The complexity of the decision is in part in such event, and that is why weak domination can be enlightened. The metric distance resumes equilibrium of all variables and a perfect solution does not exist. Generally, peach stones, cherry stones, and grape pomace achieved the most promising results for all applications in comparison to colza, softwood, or sunflower husks.

4. Conclusions

In the present research, biochar was produced from six different types of biomass in a laboratory-scale reactor of type HTF, in nitrogen, at a residence time of one hour, atmospheric pressure, and at mild temperature conditions (500 °C). Based on the experimentally measured physical and chemical features of the derived biochar, a decision-supporting tool was applied, focused on its potential role/application as biofuel, catalyst, CO_2 sequestration, and soil amendment, and as supercapacitor. The general results can be summarized as follows: (i) The effect of feedstock on biochar yield allowed to deduce a direct proportionality for the biomass lignin content and the biochar yield, e.g., the biomass having the highest lignin content—grape pomace (49.62%), showed the highest mass yield (35.07%) of biochar and vice versa for the colza and softwood. The highest HHV were obtained for the same three types of biomass (grape pomace 21.20; peach stones 22.36; cherry stones 23.62 MJ/kg) and derived biochar (grape pomace 28.11; peach stones 28.62; cherry stones 33.34 MJ/kg). As expected, the opposite was observed proportionality for the content of volatiles and fixed carbon in char, in comparison to biomass feedstock; (ii) Biochar thermal decomposition showed similar dependence on the feedstock constituents: cellulose, hemicellulose, and lignin. Two general stages were identified from the TGA/DTG analysis of biochar in air: devolatilization (stage 2)—between 180 and 560 °C, and oxidation (stage 3)—between

560 and 720 °C, accompanied by a slight shift to the higher temperatures with an increase in heating rate. The kinetic analysis confirmed that the activation energy of biochar oxidation, obtained for the devolatilization (stage 2), decreased when increasing the heating rate, except for colza and cherry stones, while during char combustion (stage 3), the opposite tendency was observed—except for cherry stones and grape pomace; (iii) Generally, all types of biochar showed considerably lower H/C and O/C ratios in comparison to biomass, thus increasing their thermal stability. The results proposed the potential use of biochar as renewable energy carriers; (iv) The SEM images showed satisfactory porosity of the particle surface, which coincided with the Specific surface area (m^2/g), S_{BET}, estimated from biochar CO_2 adsorption; (v) The experimentally measured EC and total salt content widely varied (EC from 56 to 1015 μS/cm; salt content between 28 and 980 ppm), which along with the alkaline pH (8.38–11.08) suggested further possible biochar applications as a valuable additive, enhancing the efficiency of different energy recovery technologies or even soil amendment. Biochar particular characteristics, described in Section 3.4. and Section 3.5, suggested the need of implementing a decision support analysis for determining the unrevealed application perspective of the obtained biochar; (vi) The decision support analysis showed that grape pomace, peach stones, and cherry stones achieved the most promising results for all tested applications (as biofuel, catalyst, CO_2 sequestration and soil amendment, and supercapacitor) comparatively to colza, softwood, and sunflower husks.

Supplementary Materials: The following supporting information can be downloaded at: https://www.mdpi.com/article/10.3390/app13053240/s1, Table S1: Decision support analysis for biofuel application; Table S2: Decision support analysis for catalyst application; Table S3: Decision support analysis for CO_2 sequestration and soil amendment process application; Table S4: Decision support analysis for supercapacitor process application.

Conflicts of Interest: The authors declare no conflict of interest.

References

1. Naydenova, I.; Sandov, O.; Wesenauer, F.; Laminger, T.; Winter, F. Pollutants Formation during Single Particle Combustion of Biomass under Fluidized Bed Conditions: An Experimental Study. *Fuel* **2020**, *278*, 117958. [CrossRef]

2. Petrova, T. Estimation of the Higher Heating Values for Lignocellulosic Biofuels. In Proceedings of the 2021 6th International Symposium on Environment-Friendly Energies and Applications (EFEA), Sofia, Bulgaria, 24–26 March 2021; pp. 14–18. [CrossRef]

3. Ferreira, A.F.; Ribau, J.P.; Costa, M. A Decision Support Method for Biochars Characterization from Carbonization of Grape Pomace. *Biomass Bioenergy* **2021**, *145*, 105946. [CrossRef]

4. Saidur, R.; Abdelaziz, E.A.; Demirbas, A.; Hossain, M.S.; Mekhilef, S. A Review on Biomass as a Fuel for Boilers. *Renew. Sustain. Energy Rev.* **2011**, *15*, 2262–2289. [CrossRef]

5. Demirbaş, A. Relationships between Lignin Contents and Heating Values of Biomass. *Energy Convers. Manag.* **2001**, *42*, 183–188. [CrossRef]

6. Valchev, I.; Yavorov, N.; Petrin, S. Topochemical Kinetic Mechanism of Cellulase Hydrolysis on Fast-Growing Tree Species. COST Action FP1105. *Holzforschung* **2016**, *70*, 1147–1153. [CrossRef]

7. Housseinpour, R.; Latibari, A.J.; Farnood, R.; Fatehi, P.; Sepiddehdam, S.J. Fiber Morphology and Chemical Composition of Rape-Seed (Brassica Napus) Stems. *IAWA J.* **2010**, *31*, 457–464. [CrossRef]

8. Burhenne, L.; Messmer, J.; Aicher, T.; Laborie, M.P. The Effect of the Biomass Components Lignin, Cellulose and Hemicellulose on TGA and Fixed Bed Pyrolysis. *J. Anal. Appl. Pyrolysis* **2013**, *101*, 177–184. [CrossRef]

9. Ghai, H.; Sakhuja, D.; Yadav, S.; Solanki, P.; Putatunda, C.; Bhatia, R.K.; Bhatt, A.K.; Varjani, S.; Yang, Y.-H.; Bhatia, S.K.; et al. An Overview on Co-Pyrolysis of Biodegradable and Non-Biodegradable Wastes. *Energies* **2022**, *15*, 4168. [CrossRef]

10. Mishra, S.; Upadhyay, R.K. Review on biomass gasification: Gasifiers, gasifying mediums, and operational parameters. *Mater. Sci. Energy Technol.* **2021**, *4*, 329–340. [CrossRef]

11. Alsulami, R.A.; El-Sayed, S.A.; Eltaher, M.A.; Mohammad, A.; Almitani, K.H.; Mostafa, M.E. Thermal decomposition characterization and kinetic parameters estimation for date palm wastes and their blends using TGA. *Fuel* **2023**, *334*, 126600. [CrossRef]

12. Choi, Y.-K.; Gurav, R.; Kim, H.J.; Yang, Y.-H.; Bhatia, S.K. Evaluation for Simultaneous Removal of Anionic and Cationic Dyes onto Maple Leaf-Derived Biochar Using Response Surface Methodology. *Appl. Sci.* **2020**, *10*, 2982. [CrossRef]

13. Gurav, R.; Bhatia, S.K.; Choi, T.-R.; Choi, Y.-K.; Kim, H.J.; Song, H.-S.; Park, S.L.; Lee, H.S.; Lee, S.M.; Choi, K.-Y.; et al. Adsorptive removal of crude petroleum oil from water using floating pinewood biochar decorated with coconut oil-derived fatty acids. *Sci. Total Environ.* **2021**, *781*, 146636. [CrossRef]

14. Obey, G.; Adelaide, M.; Ramaraj, R. Biochar derived from non-customized matamba fruit shell as an adsorbent for wastewater treatment. *J. Bioresour. Bioprod.* **2022**, *7*, 109–115. [CrossRef]

15. Jjagwe, J.; Olupot, P.W.; Menya, E.; Kalibbala, H.M. Synthesis and Application of Granular Activated Carbon from Biomass Waste Materials for Water Treatment: A Review. *J. Bioresour. Bioprod.* **2021**, *6*, 292–322. [CrossRef]

16. Corbin, K.R.; Hsieh, Y.S.Y.; Betts, N.S.; Byrt, C.S.; Henderson, M.; Stork, J.; DeBolt, S.; Fincher, G.B.; Burton, R.A. Grape Marc as a Source of Carbohydrates for Bioethanol: Chemical Composition, Pre-Treatment and Saccharification. *Bioresour. Technol.* **2015**, *193*, 76–83. [CrossRef] [PubMed]

17. Chiou, B.S.; Valenzuela-Medina, D.; Bilbao-Sainz, C.; Klamczynski, A.K.; Avena-Bustillos, R.J.; Milczarek, R.R.; Du, W.X.; Glenn, G.M.; Orts, W.J. Torrefaction of Pomaces and Nut Shells. *Bioresour. Technol.* **2015**, *177*, 58–65. [CrossRef]

18. Özsin, G.; Pütün, A.E. A Comparative Study on Co-Pyrolysis of Lignocellulosic Biomass with Polyethylene Terephthalate, Polystyrene, and Polyvinyl Chloride: Synergistic Effects and Product Characteristics. *J. Clean. Prod.* **2018**, *205*, 1127–1138. [CrossRef]

19. Mohamed, A.R.; Mohammadi, M.; Darzi, G.N. Preparation of Carbon Molecular Sieve from Lignocellulosic Biomass: A Review. *Renew. Sustain. Energy Rev.* **2010**, *14*, 1591–1599. [CrossRef]

20. Duman, G.; Okutucu, C.; Ucar, S.; Stahl, R.; Yanik, J. The Slow and Fast Pyrolysis of Cherry Seed. *Bioresour. Technol.* **2011**, *102*, 1869–1878. [CrossRef]

21. González, J.F.; Encinar, J.M.; Canito, J.L.; Sabio, E.; Chacón, M. Pyrolysis of Cherry Stones: Energy Uses of the Different Fractions and Kinetic Study. *J. Anal. Appl. Pyrolysis* **2003**, *67*, 165–190. [CrossRef]

22. Petrov, N.; Budinova, T.; Razvigorova, M.; Minkova, V.; Vigouroux, R.A.Z.; Bjornbom, E. Preparation of Activated Carbons from Cherry Stones, Apricot Stones and Grape Seeds for Removal of Metal Ions from Water. In Proceedings of the 2nd Olle Indstorm Symposium on Renewable Energy-Bioenergy, Stockholm, Sweden, 9–11 June 1999; pp. 46–50.

23. Pedras, B.M.d.S. Valorization of Grape Pomace through Hot Compressed Water Extraction/Hydrolysis. Master's Thesis, Universidade Nova, Lisbon, Portugal, 2015. Available online: https://run.unl.pt/handle/10362/16225 (accessed on 27 February 2023).

24. Bhatia, S.K.; Palai, A.K.; Kumar, A.; Bhatia, R.K.; Patel, A.K.; Thakur, V.K.; Yang, Y.-H. Trends in renewable energy production employing biomass-based biochar. *Bioresour. Technol.* **2021**, *340*, 125644. [CrossRef]

25. Novotný, M.; Marković, M.; Raček, J.; Šipka, M.; Chorazy, T.; Tošić, I.; Hlavínek, P. The use of biochar made from biomass and biosolids as a substrate for green infrastructure: A review. *Sustain. Chem. Pharm.* **2023**, *32*, 100999. [CrossRef]

26. Qian, S.; Zhou, X.; Fu, Y.; Song, B.; Yan, H.; Chen, Z.; Sun, Q.; Ye, H.; Qin, L.; Lai, C. Biochar-compost as a new option for soil improvement: Application in various problem soils. *Sci. Total Environ.* **2023**, *870*, 162024. [CrossRef] [PubMed]

27. Das, S.; Mohanty, S.; Sahu, G.; Rana, M.; Pilli, K. Biochar: A Sustainable Approach for Improving Soil Health and Environment. In *Soil Erosion-Current Challenges and Future Perspectives in a Changing World*; IntechOpen: London, UK, 2021. [CrossRef]

28. Sun, W.; Zhang, S.; Su, C. Impact of Biochar on the Bioremediation and Phytoremediation of Heavy Metal(loid)s in Soil. In *Advances in Bioremediation and Phytoremediation*; InTech: Rijeka, Croatia, 2018. [CrossRef]

29. Sharma, G.K.; Jena, R.K.; Hota, S.; Kumar, A.; Ray, P.; Fagodiya, R.K.; Malav, L.C.; Yadav, K.K.; Gupta, D.K.; Khan, S.A.; et al. Recent Development in Bioremediation of Soil Pollutants through Biochar for Environmental Sustainability. In *Biochar Applications in Agriculture and Environment Management*; Singh, J., Singh, C., Eds.; Springer: Cham, Switzerland, 2020. [CrossRef]

30. Jung, S.; Kim, M.; Kim, Y.-H.; Lin, K.-Y.A.; Chen, W.-H.; Tsang, Y.F.; Kwon, E.E. Use of sewage sludge biochar as a catalyst in production of biodiesel through thermally induced transesterification. *Biochar* **2022**, *4*, 67. [CrossRef]

31. Kumar, S.; Soomro, S.A.; Harijan, K.; Uqaili, M.A.; Kumar, L. Advancements of Biochar-Based Catalyst for Improved Production of Biodiesel: A Comprehensive Review. *Energies* **2023**, *16*, 644. [CrossRef]

32. Arenas, C.; Sotres, A.; Alonso, R.M.; González-Arias, J.; Morán, A.; Gómez, X. Pyrolysed almond shells used as electrodes in microbial electrolysis cell. *Biomass Convers. Biorefinery* **2022**, *12*, 313–321. [CrossRef]

33. Chen, C.; Zhang, M.; Chen, X.; Yan, J.; Li, H.; Xu, X. Electricity production and pollutant removal performance of walnut shell biochar electrode in microbial fuel cell. *Chin. J. Environ. Eng.* **2022**, *16*, 3281–3290. [CrossRef]

34. Piyo, N. Liquefaction of Sunflower Husks for Biochar Production. Master's Thesis, North-West University, Vanderbijlpark, Portugal, 2014. Available online: https://repository.nwu.ac.za/bitstream/handle/10394/11942/Piyo_N.pdf?sequence=1 (accessed on 27 February 2023).

35. Demirbaş, A. Calculation of Higher Heating Values of Biomass Fuels. *Fuel* **1997**, *76*, 431–434. [CrossRef]

36. López-González, D.; Fernandez-Lopez, M.; Valverde, J.L.; Sanchez-Silva, L. Thermogravimetric-Mass Spectrometric Analysis on Combustion of Lignocellulosic Biomass. *Bioresour. Technol.* **2013**, *143*, 562–574. [CrossRef]

37. Fan, F.; Zheng, Y.; Huang, Y.; Lu, Y.; Wang, Z.; Chen, B.; Zheng, Z. Combustion Kinetics of Biochar Prepared by Pyrolysis of Macadamia Shells. *BioResources* **2017**, *12*, 3918–3932. [CrossRef]

38. Suman, S.; Gautam, S. Biochar Derived from Agricultural Waste Biomass Act as a Clean and Alternative Energy Source of Fossil Fuel Inputs. In *Energy Systems and Environment*; IntechOpen: London, UK, 2018. [CrossRef]

39. Ferreira, A.F.; Soares Dias, A.P.; Silva, C.M.; Costa, M. Evaluation of Thermochemical Properties of Raw and Extracted Microalgae. *Energy* **2015**, *92*, 365–372. [CrossRef]

40. *No ISO 18134-3:2015*; Solid Biofuels—Determination of Moisture Content—Oven Dry Method—Part 3: Moisture in General Analysis Sample. ISO: London, UK, 2015.

41. *ISO 18122:2015*; Solid Biofuels–Determination of Ash Content. ISO: London, UK, 2015.

42. *ISO 18123:2015*; Solid Biofuels—Determination of the Content of Volatile Matter. ISO: London, UK, 2015.

43. *J.19P, S. EN 14918:2010*; Solid Biofuels-Determination of Calorific Value. CSA: Singapore, 2010.

44. Singh, B.; Dolk, M.M.; Shen, Q.; Camps-Arbestain, M. Biochar PH, Electrical Conductivity and Liming Potential. In *Biochar: A Guide to Analytical Methods*; CSIRO: Canberra, Australia, 2017; pp. 23–38.

45. López-González, D.; Fernandez-Lopez, M.; Valverde, J.L.; Sanchez-Silva, L. Kinetic Analysis and Thermal Characterization of the Microalgae Combustion Process by Thermal Analysis Coupled to Mass Spectrometry. *Appl. Energy* **2014**, *114*, 227–237. [CrossRef]

46. Liu, N.A.; Fan, W.; Dobashi, R.; Huang, L. Kinetic Modeling of Thermal Decomposition of Natural Cellulosic Materials in Air Atmosphere. *J. Anal. Appl. Pyrolysis* **2002**, *63*, 303–325. [CrossRef]

47. Wang, X.; Zhai, M.; Wang, Z.; Dong, P.; Lv, W.; Liu, R. Carbonization and Combustion Characteristics of Palm Fiber. *Fuel* **2018**, *227*, 21–26. [CrossRef]

48. Abdullah, H.; Wu, H. Biochar as a Fuel: 1. Properties and Grindability of Biochars Produced from the Pyrolysis of Mallee Wood under Slow-Heating Conditions. *Energy Fuels* **2009**, *23*, 4174–4181. [CrossRef]

49. Lee, J.; Kim, K.H.; Kwon, E.E. Biochar as a Catalyst. *Renew. Sustain. Energy Rev.* **2017**, *77*, 70–79. [CrossRef]

50. Cheng, F.; Li, X. Preparation and Application of Biochar-Based Catalysts for Biofuel Production. *Catalysts* **2018**, *8*, 346. [CrossRef]

51. Li, X.; Zhang, J.; Liu, B.; Su, Z. A Critical Review on the Application and Recent Developments of Post-Modified Biochar in Supercapacitors. *J. Clean. Prod.* **2021**, *310*, 127428. [CrossRef]

52. Deb, K. *Multi-Objective Optimization Using Evolutionary Algorithms*; Wiley Interscience Series in Systems and Optimization; John Wiley & Sons: New York, NY, USA, 2001; ISBN 978-0-471-87339-6.

53. Gao, Y.; Wang, X.; Chen, Y.; Li, P.; Liu, H.; Chen, H. Pyrolysis of Rapeseed Stalk: Influence of Temperature on Product Characteristics and Economic Costs. *Energy* **2017**, *122*, 482–491. [CrossRef]

54. Khiari, B.; Jeguirim, M. Pyrolysis of Grape Marc from Tunisian Wine Industry: Feedstock Characterization, Thermal Degradation and Kinetic Analysis. *Energies* **2018**, *11*, 730. [CrossRef]

55. Ronsse, F.; van Hecke, S.; Dickinson, D.; Prins, W. Production and Characterization of Slow Pyrolysis Biochar: Influence of Feedstock Type and Pyrolysis Conditions. *GCB Bioenergy* **2012**, *5*, 104–115. [CrossRef]

56. Wystalska, K.; Malińska, K.; Włodarczyk, R.; Chajczyk, O. Effects of Pyrolysis Parameters on the Yield and Properties of Biochar from Pelletized Sunflower Husk. *E3S Web Conf.* **2018**, *44*, 00197. [CrossRef]

57. Zabaniotou, A.A.; Kantarelis, E.K.; Theodoropoulos, D.C. Sunflower Shells Utilization for Energetic Purposes in an Integrated Approach of Energy Crops: Laboratory Study Pyrolysis and Kinetics. *Bioresour. Technol.* **2008**, *99*, 3174–3181. [CrossRef] [PubMed]

58. Anabel, F.; Celia, R.; Germán, M.; Rosa, R. Determination of Effective Moisture Diffusivity and Thermodynamic Properties Variation of Regional Wastes under Different Atmospheres. *Case Stud. Therm. Eng.* **2018**, *12*, 248–257. [CrossRef]

59. Boukaous, N.; Abdelouahed, L.; Chikhi, M.; Meniai, A.H.; Mohabeer, C.; Bechara, T. Combustion of Flax Shives, Beech Wood, Pure Woody Pseudo-Components and Their Chars: A Thermal and Kinetic Study. *Energies* **2018**, *11*, 2146. [CrossRef]

60. Fu, P.; Yi, W.; Bai, X.; Li, Z.; Hu, S.; Xiang, J. Effect of Temperature on Gas Composition and Char Structural Features of Pyrolyzed Agricultural Residues. *Bioresour. Technol.* **2011**, *102*, 8211–8219. [CrossRef] [PubMed]
61. Botelho, T.; Costa, M.; Wilk, M.; Magdziarz, A. Evaluation of the Combustion Characteristics of Raw and Torrefied Grape Pomace in a Thermogravimetric Analyzer and in a Drop Tube Furnace. *Fuel* **2018**, *212*, 95–100. [CrossRef]
62. Petrović, J.; Perišić, N.; Maksimović, J.D.; Maksimović, V.; Kragović, M.; Stojanović, M.; Laušević, M.; Mihajlović, M. Hydrothermal Conversion of Grape Pomace: Detailed Characterization of Obtained Hydrochar and Liquid Phase. *J. Anal. Appl. Pyrolysis* **2016**, *118*, 267–277. [CrossRef]
63. Colantoni, A.; Evic, N.; Lord, R.; Retschitzegger, S.; Proto, A.R.; Gallucci, F.; Monarca, D. Characterization of Biochars Produced from Pyrolysis of Pelletized Agricultural Residues. *Renew. Sustain. Energy Rev.* **2016**, *64*, 187–194. [CrossRef]
64. Van Krevelen, D.W.; Te Nijenhuis, K. *Properties of Polymers: Their Correlation with Chemical Structure; Their Numerical Estimation and Prediction from Additive Group Contributions*, 4th ed.; Elsevier: Amsterdam, The Netherlands, 2009; ISBN 978-0-08-054819-7.
65. Misse, S.E.; Brillard, A.; Mayandyshev, P.; Brilhac, J.F.; Obonou, M. Comparative Pyrolysis, Combustion, and Kinetic Modeling of Twelve Cameroonian Woody Biomass. *Biomass Convers. Biorefinery* **2022**, *12*, 3161–3181. [CrossRef]
66. Oliveira, F.R.; Patel, A.K.; Jaisi, D.P.; Adhikari, S.; Lu, H.; Khanal, S.K. Environmental Application of Biochar: Current Status and Perspectives. *Bioresour. Technol.* **2017**, *246*, 110–122. [CrossRef] [PubMed]
67. Waqas, M.; Aburiazaiza, A.S.; Miandad, R.; Rehan, M.; Barakat, M.A.; Nizami, A.S. Development of Biochar as Fuel and Catalyst in Energy Recovery Technologies. *J. Clean. Prod.* **2018**, *188*, 477–488. [CrossRef]
68. Leng, L.; Huang, H.; Li, H.; Li, J.; Zhou, W. Biochar Stability Assessment Methods: A Review. *Sci. Total Environ.* **2019**, *647*, 210–222. [CrossRef]
69. Crombie, K.; Mašek, O.; Sohi, S.P.; Brownsort, P.; Cross, A. The Effect of Pyrolysis Conditions on Biochar Stability as Determined by Three Methods. *GCB Bioenergy* **2013**, *5*, 122–131. [CrossRef]
70. Pala, M.; Kantarli, I.C.; Buyukisik, H.B.; Yanik, J. Hydrothermal Carbonization and Torrefaction of Grape Pomace: A Comparative Evaluation. *Bioresour. Technol.* **2014**, *161*, 255–262. [CrossRef]
71. Marczak, M.; Karczewski, M.; Makowska, D.; Burmistrz, P. Impact of the Temperature of Waste Biomass Pyrolysis on the Quality of the Obtained Biochar. *Agric. Eng.* **2016**, *20*, 115–124. [CrossRef]
72. Yavorov, N.; Petrin, S.; Valchev, I.; Nenkova, S. Potential of Fast Growing Poplar, Willow and Paulownia for Bioenergy Production. *Bulg. Chem. Commun.* **2015**, *47*, 5–9.
73. Dhyani, V.; Bhaskar, T. A Comprehensive Review on the Pyrolysis of Lignocellulosic Biomass. *Renew. Energy* **2018**, *129*, 695–716. [CrossRef]
74. Angın, D. Effect of Pyrolysis Temperature and Heating Rate on Biochar Obtained from Pyrolysis of Safflower Seed Press Cake. *Bioresour. Technol.* **2013**, *128*, 593–597. [CrossRef]
75. Nzediegwu, C.; Arshad, M.; Ulah, A.; Naeth, M.A.; Chang, S.X. Fuel, Thermal and Surface Properties of Microwave-Pyrolyzed Biochars Depend on Feedstock Type and Pyrolysis Temperature. *Bioresour. Technol.* **2021**, *320*, 124282. [CrossRef]
76. Manyà, J.J.; González, B.; Azuara, M.; Arner, G. Ultra-Microporous Adsorbents Prepared from Vine Shoots-Derived Biochar with High CO_2 Uptake and CO_2/N_2 Selectivity. *Chem. Eng. J.* **2018**, *345*, 631–639. [CrossRef]
77. Vassilev, S.V.; Vassileva, C.G.; Song, Y.C.; Li, W.Y.; Feng, J. Ash Contents and Ash-Forming Elements of Biomass and Their Significance for Solid Biofuel Combustion. *Fuel* **2017**, *208*, 377–409. [CrossRef]
78. Obernberger, I.; Brunner, T.; Bärnthaler, G. Chemical Properties of Solid Biofuels-Significance and Impact. *Biomass Bioenergy* **2006**, *30*, 973–982. [CrossRef]
79. Anjum, M.; Miandad, R.; Waqas, M.; Tarar, A.I.; Alafif, Z.; Aburiazaiza, A.S.; Barakat, M.A.; Akhtar, T. Solid Waste Management in Saudi Arabia: A Review. *J. Appl. Agric. Biotechnol.* **2016**, *1*, 13–26.
80. Mohamed, M.; Yusup, S.; Bustam, M.A. Synthesis of CaO-Based Sorbent from Biomass for CO_2 Capture in Series of Calcination-Carbonation Cycle. *Procedia Eng.* **2016**, *148*, 78–85. [CrossRef]
81. Conder, J.; Fic, K.; Ghimbeu, C.M. Supercapacitors (Electrochemical Capacitors). In *Char and Carbon Materials Derived from Biomass: Production, Characterization and Applications*; Elsevier: Amsterdam, The Netherlands, 2019; pp. 383–427. [CrossRef]
82. Brassard, P.; Godbout, S.; Lévesque, V.; Palacios, J.H.; Raghavan, V.; Ahmed, A.; Hogue, R.; Jeanne, T.; Verma, M. 4-Biochar for Soil Amendment. In *Char and Carbon Materials Derived from Biomass: Production, Characterization and Applications*; Elsevier: Amsterdam, The Netherlands, 2019; pp. 109–146. ISBN 9780128148938. [CrossRef]
83. EBC. *European Biochar Certificate-Guidelines for a Sustainable Production of Biochar*; Version 6.2E of 04th February 2016; Guidelines European Biochar Certificate for a Sustainable Production of Biochar 2; European Biochar Foundation (EBC): Arbaz, Switzerland, 2012; Available online: http://www.european-biochar.org/en/download (accessed on 27 February 2023). [CrossRef]
84. Racioppi, M.; Tartaglia, M.; de la Rosa, J.M.; Marra, M.; Lopez-Capel, E.; Rocco, M. Response of Ancient and Modern Wheat Varieties to Biochar Application: Effect on Hormone and Gene Expression Involved in Germination and Growth. *Agronomy* **2020**, *10*, 5. [CrossRef]